

Kent Academic Repository

Full text document (pdf)

Citation for published version

Jun, S. and Elibiary, Ahmed and Sanz-Izquierdo, Benito and Winchester, L. and Bird, D. and McClelland, A. (2018) 3D Printing of Conformal Antennas for Diversity Wrist Worn Applications. IEEE Transactions on Components, Packaging and Manufacturing Technology . ISSN 2156-3950.

DOI

<https://doi.org/10.1109/TCPMT.2018.2874424>

Link to record in KAR

<https://kar.kent.ac.uk/69895/>

Document Version

Author's Accepted Manuscript

Copyright & reuse

Content in the Kent Academic Repository is made available for research purposes. Unless otherwise stated all content is protected by copyright and in the absence of an open licence (eg Creative Commons), permissions for further reuse of content should be sought from the publisher, author or other copyright holder.

Versions of research

The version in the Kent Academic Repository may differ from the final published version.

Users are advised to check <http://kar.kent.ac.uk> for the status of the paper. **Users should always cite the published version of record.**

Enquiries

For any further enquiries regarding the licence status of this document, please contact:

researchsupport@kent.ac.uk

If you believe this document infringes copyright then please contact the KAR admin team with the take-down information provided at <http://kar.kent.ac.uk/contact.html>

3D Printing of Conformal Antennas for Diversity Wrist Worn Applications

S. Jun, A. Elibiary, B.Sanz-Izquierdo, L. Winchester, D. Bird, A. McClelland

Abstract—This paper presents for the first time the application of 3D printing techniques for the development of conformal antennas for diversity wrist worn wireless communications. Three processes are described with the common challenge of depositing the metallic layers of the antennas on a bracelet fabricated using fuse filament fabrication (FFF). The first is a multistep process which combines adding a layer to smooth the surface of the band, aerosol jetting the metallic tracks, flash curing and then electroplating. The second combines painting the metallic layers by hand and then electroplating. The last process uses a single machine to fabricate both the bracelet and then the metallic layers by means of a direct write system with silver conductive ink. The wrist worn antennas are presented and its performances on the human wrist are discussed. All antennas cover 2.4 GHz and 5.5 GHz used for WLAN communication with the reflection coefficients less than -10 dB. The diversity wrist worn antennas system is developed for the final two processes. Three WLAN antennas are fabricated at different positions and shape angles within the bracelet. In terms of communications systems, the advantage of this configuration is that it can increase coverage. The radiation patterns of the antenna are nearly omnidirectional in free space and directional on the human wrist. When the patterns of the three antennas are combined together, the coverage for the communication system improves. Simulation results of all antenna designs and studies using the finite integration technique (FIT) agree well with experimental measurement results. The main motivation of this work is to investigate alternative additive manufacturing methods for the development of conformal diversity antennas on customized 3D printed parts.

Index Terms— Additive manufacturing, 3D printing, Bracelet antenna, Diversity, Wrist worn application.

I. INTRODUCTION

RECENTLY, additive manufacturing (AM) or 3D printing (3DP) has become a popular topic in the research and development community. This trend has been supported by the expiration of patents related to AM and 3DP technology and the increasing availability of new AM machines and processes

This work was supported by UK EPSRC High Value Manufacturing Fellowship (REF: EP/L017121/1), Royal Academy of Engineering Industrial Secondment scheme (REF: ISS1617/48) and Royal Society research grant (REF: RG 130637)

S. Jun, A. Elibiary, and B. Sanz-Izquierdo, are with the School of Engineering and Digital Arts, University of Kent, Canterbury CT2 7NT, U.K. (e-mail: sj329@kent.ac.uk; b.sanz@kent.ac.uk; e.a.parker@kent.ac.uk).

L. Winchester, D. Bird and A. McClelland are with the Centre for Process Innovation (CPI) Thomas Wright Way, Netpark, Sedgefield TS21 3FG, U.K. (e-mail: David.Bird@uk-cpi.com, Alan.McClelland@uk-cpi.com).

[1]-[3]. AM can provide many benefits such as the reductions in cost and the time, personal customization and complex shaped manufacturing [4]. The area of radio frequency (RF) and microwave engineering can greatly benefit by the use of AM. For example, 3DP can be used for the development of new and sometimes complex 3D antenna structures [5] - [13]. Novel 3D frequency selective structures have been developed by printing the elements of the array in [5]. Manufacturing consideration for the printing 3D fractal antennas are discussed in [6]. 3D printed patch antenna with an embedded wire mesh is presented and characterized in [7]. 3D printed cube antennas for wireless sensor applications are introduced in [8]. An electrical meander line antenna fabricated on the conformal glass substrate is discussed in [9]. A circularly polarized patch antenna has been fabricated by using low cost inkjet and 3D printing techniques in [10].

3DP has also found applications in the development of wearable garments and devices [11]-[15]. Antennas are needed if these wearables are smart and wireless connected. Ideally, these antennas should be printed along the wearable structure. A novel loop antenna for wearable applications has been realized by using a flexible 3D printable material in [13]. A dual band CPW fed antenna has been printed on leather substrate for foot wear application in [14]. An inkjet printing method on textiles for wearable antenna is presented in [15].

Antenna diversity is an important technique in advanced microwave wireless and mobile communication systems. Antenna diversity can improve performance and wireless transmission in environments with multipath fading of radio waves [16], [17]. Multipath signal fading causes the restriction in system channel capacity. Body worn systems can benefit from antenna diversity. It can improve channel capacity, compensate for some of the human body effects such as loss in antenna matching, radiation efficiency and blocking of the signal from the human body movements [18] - [21].

This paper presents the 3D printing of conformal antennas for wrist worn applications. It proposes manufacturing processes to address the challenges related to the 3D printing of antennas on a curved substrate that has been fabricated using inexpensive fuse filament fabrication techniques (FFF). The main issues relate to the surface roughness and surface energy of the FFF substrates [22]. On the other hand, wrist worn devices such as wristbands and bracelets are made of curved surfaces and require a procedure that is able to print in such shapes. Three additive fabrication processes have been assessed and are discussed here. The first is a multi-step process that is able to smooth the surface and then add metallic layers on a curved

bracelet. The second involves painting the antennas on the bracelet and then electroplating. The last uses a machine to fabricate both the antenna and the bracelet. This paper is organized as follows. Section II describes the basic antenna design and the development of a diversity antenna systems on the bracelet. Section III describes the three fabrication methods investigated and analyses the corresponding measurement results. Finally, section IV summarizes all the results, compares the different techniques used and provides some conclusions. All antenna designs have been simulated using CST Microwave Studio™ and verified with experimental results.

II. WRIST WORN ANTENNA DESIGN

A. Antenna design and Analysis

The dipole antenna is one of the simplest radiating structures that can be used for the testing of fabrication processes [23], [24]. It is also suitable for evaluation the effect of human body on antenna performance [11], [25]. Fig. 1 shows the configuration of the dipole antenna with two resonant arms at each end on the 3D bracelet. The inner radii of the elliptical bracelet substrate are 35 and 30 mm and the thickness 3 mm. The dimensions have been chosen using the first author's wrist. Low-cost polylactic acid plastic filament (PLA) material with dielectric constant of $\epsilon_r = 2.4$, loss tangent of $\tan\delta = 0.01$ is employed as substrate [26]. Each dipole arm has two sections, the longer (L) for the 2.4 GHz and the shorter (S) for the 5.5 GHz WLAN bands. The final dimensions of the antenna are as followed: $A = 42.4$ mm, $B = 9$ mm, $S = 9$ mm, $L = 24$ mm, $G = 0.4$ mm, $T = 2$ mm. Both the conformal antenna in Fig. 1 (a) and the corresponding flat antenna (Fig. 1 (b)) meet the WLAN bands. Only the input matching at higher band is slightly sensitive to bending the flat structure.

The potential effect of fabrication errors to changes in impedance matching (S_{11}) is shown in Fig. 2. The length of the two main arms, L and S, are the most likely dimensions to cause a change in resonant frequency of the antenna. The longer arms, L, controls the lower frequency while the second resonator, S, tunes the higher frequency. The antenna is required to cover the 2.4 GHz to 2.5 GHz band 5.0 GHz to 6 GHz bands with an S_{11} of less than -10 dB. Using this target, the maximum variations allowed are 2 mm (3%) and 1 mm (5%) for the larger (L) and smaller (S) resonators respectively. This is considered to be acceptable for the resolution of the techniques that are described in this paper. The thickness in the z-axis of the metallic tracks may also vary during a additive manufacturing process but this was found to have a marginal effect on S_{11} for values of less than 200 μm .

The high relative permittivity of the human body produces a shift in the resonance frequency and reduces antenna efficiency [19]. Therefore, a wrist worn antenna should also be considered with the presence of the human wrist. A three tissue body model is typically employed to emulate this. Fig. 3(a) shows a cross section of the antenna and bracelet mounted on the elliptical non-homogenous human tissue layers with dimensions of the skin (1 mm), fat (2 mm) and muscle (29 mm). The length of the piece of wrist used for the simulation is 24 mm. The electrical parameters of human tissue layers are given in Table I [27].

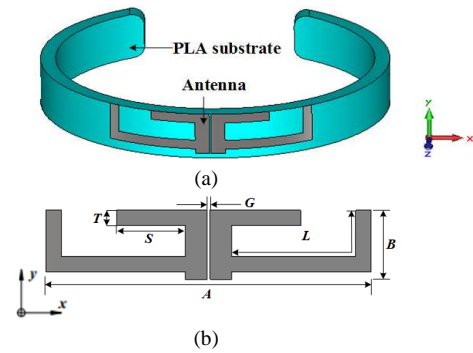


Fig. 1 Configuration of the wrist worn antenna on the bracelet substrate (a) perspective view (b) dimension.

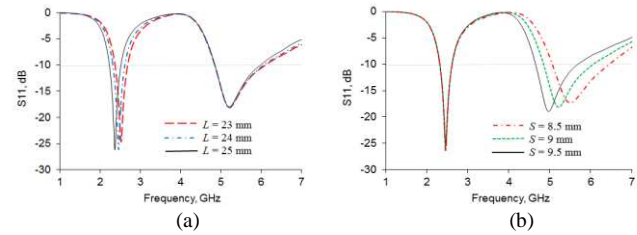


Fig. 2. Computed sensitivity of the antenna to changes in the dimensions (a) length L (b) length S on reflection coefficient (S_{11}).

Fig. 3(b) presents the simulated reflection coefficient (S_{11}) of the proposed antenna for variations of the distance between the bracelet and the human body from 0 to 3 mm, and also free space. The resonant frequencies of the lower and higher bands are shifted to the left as the gap decreases. The bandwidth of the higher frequency also becomes wider.

The difference in radiation patterns for the two cases (with vs without human wrist model) is shown in Fig. 3(c). The human body reduces significantly the back radiating power. This reduction may cause insufficient coverage the wireless communications. This coverage can be improved by adding more antennas in the bracelet as described below.

B. Diversity Antenna System

Multiple antennas are typically required to increase coverage in the communication system. This type of antenna arrangement is typically defined as space diversity. Fig. 4 shows a simple antenna diversity solution for the bracelet. Two more antennas have been added symmetrically at a distance of 50.3 mm from the antenna in the center. The idea is that each antenna may be connected to its own RF circuit and circuit board and is able to send information such as location about the person with the bracelet. Fig. 5 shows the main S parameters of the three antennas in free space and with human body. All antennas cover 2.4 GHz and 5.5 GHz frequency bands with S_{ii} less than -10 dB. There is also good isolation between the antennas as indicated by the S_{ij} parameters (S_{12} , S_{21} , S_{23} , S_{32} , S_{31} , S_{13}) with levels of less than -10 dB.

Fig. 6 shows the simulated radiation pattern (x-z plane) at 2.4 GHz and 5.5 GHz with human body. There is a clear increase in coverage compared with just one antenna as indicated by the additional power available at 45° , 135° , 225° , and 315° . Due to the presence of the human body, the backward direction is distorted and reduced. However, the three radiation patterns generated improves coverage. The performance of the pattern diversity system provides stable communication in all direction for the transmitting or receiving signals.

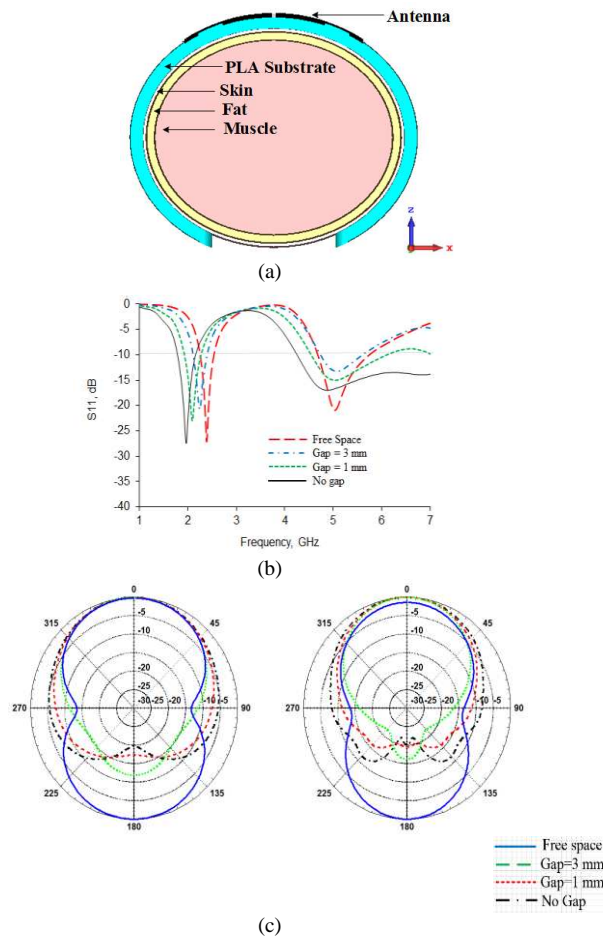


Fig. 3. Human wrist model with the wrist wear antenna and effect on antenna performance (a) geometry (b) reflection coefficient (S_{11}) (c) radiation pattern x-z plane. (Left: 2.4 GHz, Right: 5.5 GHz).

TABLE I
HUMAN TISSUE LAYERS

	Relative Permittivity		Conductivity	
	2.4 GHz	5.5 GHz	2.4 GHz	5.5 GHz
Skin	38	35.3	1.4	3.4
Fat	5.2	4.9	0.1	0.2
Muscle	52.7	48.8	1.7	4.6

III. ADDITIVE MANUFACTURING METHODS INVESTIGATED

A. Optomec's Aerosol Jet Technology

The first process tested is the fabrication of the bracelet using fuse filament fabrication [11] and then the tracks of the antenna deposited with Optomec's Aerosol Jet technology [22]. In order to start the fabrication process, the digital model of the bracelet was exported from CST Microwave Studio™ to an STL file. It was then sent to an Ultimaker 3D printer using CURA software. The density of the print was set to 100%. White PLA was employed to make the bracelet. Preliminary experiments using Optomec's Aerosol Jet to deposit layers directly on the bracelet were unsuccessful. This was due to problems related to the surface properties of the PLA substrate [22], with the surface roughness described in the range of 10 μ m to 40 μ m in [28]. Consequently, a new process was developed and is fully illustrated in Fig. 7.

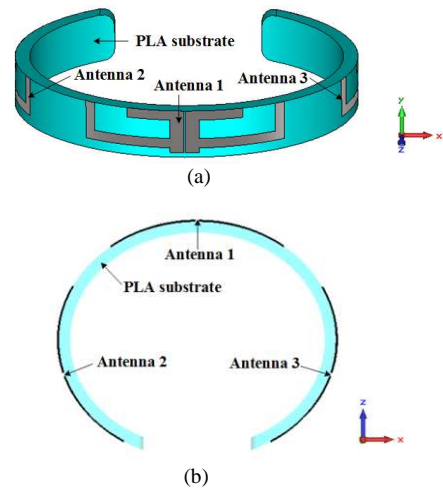


Fig. 4. Configuration of the diversity wrist worn antenna (a) prospective view (b) top side.

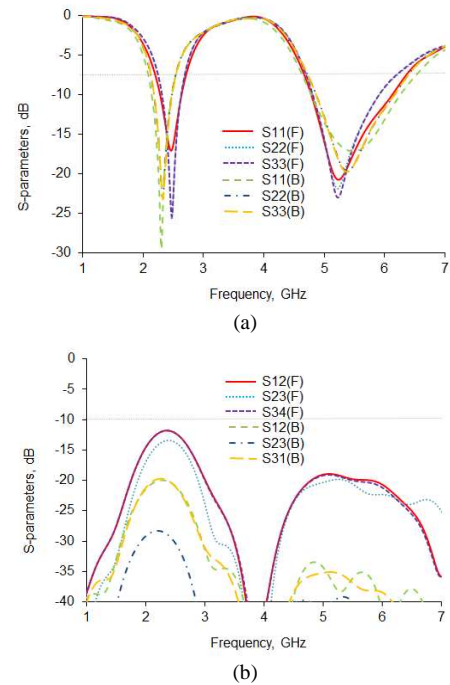


Fig. 5. Simulated S-parameters of the proposed diversity wrist worn antenna (a) reflection coefficients (b) correlation coefficients. (F: Free space, B: Human body)

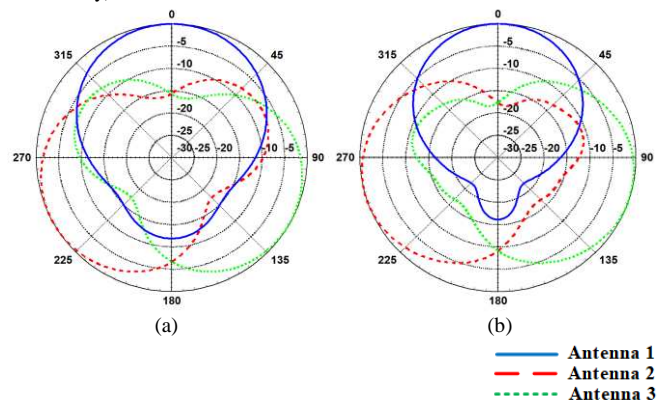


Fig. 6. Radiation patterns of the diversity wrist worn antenna on the human body at (a) 2.4 GHz (b) 5.5 GHz.

A layer of fast-acting adhesive (Cyanoacrylates) was deposited to smooth the FFF surface and also increase the surface energy. Only then the metallic layers were added uniformly using Optomec's aerosol jetting process with Cabot CS-32 silver conductive ink. The thickness of the printed silver ink layer was about 20 μm . Owing to the low-temperature characteristics of the FFF substrate, the antenna was cured using a NovaCentrix PulseForge machine [29] in the Centre for Process Innovation (CPI) [30]. The printed antenna was then electroplated to further increase the conductivity. This added layer of copper was about 50 μm . Fig. 8(a) and Fig. 8(b) show the photograph of the fabricated antennas before and after electroplating process. A 50 ohm SMA connector was attached to the antenna. Fig. 9 shows the surface profile of the printed plastic after the smoothing layer, and also the printed ink layer. The calculation of the surface roughness was done on a TalySurf CCI which provides ultra-high resolution interferometric measurements for non-contact surface roughness. The printed plastic PLA with the layer of glue had a surface roughness of about 5 μm . The surface roughness of the silver ink was about 1 μm which is significantly smoother than the PLA. This indicates that when the ink is deposited onto the plastic, it levels out, filling in most of the gaps along the surface. The electro plating procedure contributes further to this smoothing process.

S_{11} measurements were carried out using an Anritsu 37397C vector network analyzer. A gap from the human wrist to the antenna was set to approximately 5 mm using polystyrene formers. Fig. 10 presents the measured S_{11} of the wrist worn antenna. The 2.4 GHz and 5.5 GHz bands are covered with an S_{11} level of less than -10 dB. Some differences are observed at the higher band compared with simulations (Fig.5 (a)). This is probably due to connectors, cabling effects and fabrication errors. Fig. 11 shows the measured radiation patterns at 2.4 GHz and 5.5 GHz. Both results show omnidirectional radiation patterns in free space, and mainly directional on the human wrist.

Although this first method was successful, the main drawback was the many processes required for the fabrication of the antenna. Another problem was the fact that the machine used in the jetting process was only able to move in the x-y axis and therefore calculations had to be done to produce the curved design. A 3 axis robotic arm would be ideal, but this solution could prove even more costly. In terms of antenna performance, there is a clear limitation as the body reduces significantly the power transmitted backwards and therefore communication coverage. Multiple antenna systems are desirable.

B. Fabrication of diversity antenna systems by painting and electroplating

As aforementioned, there are cases where multiple antennas might be required. These can be prototyped using a relatively simple fabrication process of the antenna by combining silver conductive paint and an electroplating process. This is illustrated in Fig. 12. First, the bracelet was printed with thin grooves of thickness of 0.2 mm. This groove facilitated the painting of the antennas. Then silver conductive ink (RS 186-3600 [31]) was applied to the substrate by hand. This ink did not provide sufficient conductivity for low temperature curing. Therefore, a layer of copper of about 50 μm was deposited by electroplating.

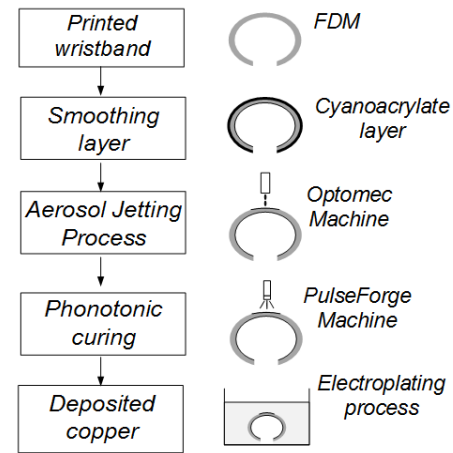


Fig. 7. Fabrication process involving aerosol jetting and electroplating

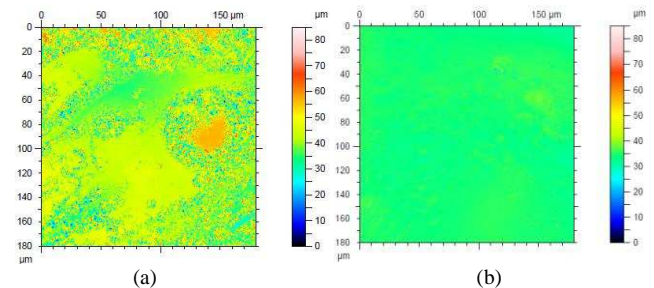


(a)



(b)

Fig. 8. Fabricated antenna on the 3D printed bracelet (a) before electroplating (b) after electroplating and with human wrist.



(a)

(b)

Fig. 9. Surface profile map of the 3D printed bracelet (a) PLA substrate after the smoothing layer was applied, and (b) the top metallic layer.

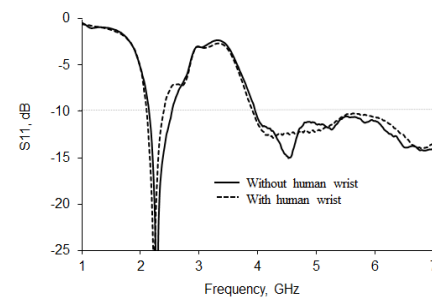


Fig. 10. Reflection coefficient (S_{11}) of the antenna fabricated with Optomec's Aerosol Jet technology

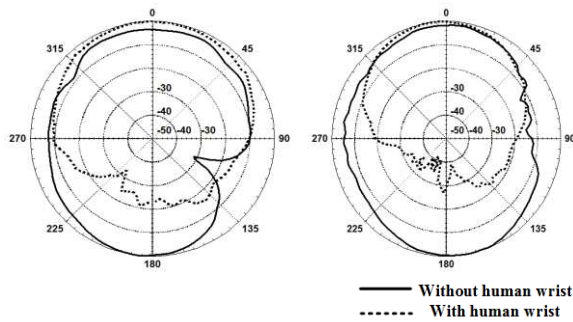


Fig. 11. Radiation pattern (Left: 2.4 GHz, Right: 5.5 GHz)

Fig. 13 shows the surface profile of the printed layers. The surface roughness of the PLA substrate was about $10\ \mu\text{m}$ while the roughness for the copper layer was about $3\ \mu\text{m}$. Fig. 14 shows the measured S parameter on the human body. Although the S parameters differed between ports, the antennas are able to cover the intended frequency bands. The differences in S parameters for various ports is probably due to the variation in distances between the antennas and the human body. These variations are likely to occur in real life scenarios. The presence of a new mode at about 6.8GHz compared with the simulations (Fig.5 (a)) could be due the effect of cables and connectors. Imperfect ledges due to the painting by hand may also be a factor. Fig. 15 presents the set up for the far field measurements of the antenna with the human wrist. Two scenarios of hand up and hand down were tested. Fig. 16 and Fig. 17 present the measured radiation patterns for the two cases. The measured gain at 2.4 GHz and 5.5 GHz was 2.0 dB and 1.3 dB respectively. As seen in the results, both scenarios provided directional radiation pattern on the human body. In the hand up case, the back side of radiation pattern is suppressed only by the human arm. Whereas, in the hand down case, the back side of the radiation pattern is further blocked by the rest of the human body. As expected, the case of the hand down has slightly more backside radiation suppression than the one with the hand up.

C. Full 3D printing using an open-Source FFF machine and a pneumatic dispenser

The final fabrication technique tested uses a single machine that combines two technologies: FFF and direct write. In order to realize such process, a machine was developed in-house using the open-source Mbot Cube [32] printer as a base frame. A direct drive extruder was used for the FFF fabrication while a pneumatic dispenser the direct write technique. The Techcon TS250 pneumatic dispenser [33] with output pressure of between 1 - 100 psi was employed. The dispenser was connected to a syringe with a $250\ \mu\text{m}$ nozzle to deposit variable line widths of silver ink. The machine with the syringe, dispenser, and the plastic extruder are shown in Fig. 18(a). The dispenser was operated using a serial switch. This connected the printers' microcontroller board to the input trigger of the dispenser. By using a mixture of stepper signals from the RAMPS board, an Arduino was used to turn on or off the dispenser. The dispenser was capable of depositing a layer thickness of less than $200\ \mu\text{m}$ of the silver conductive ink. The silver conductive ink was provided by Voxel8 [33]. The conductivity as stated by the manufacturer is about less than $5.0 \times 10^{-7}\ \Omega\text{-m}$ which makes it highly conductive.

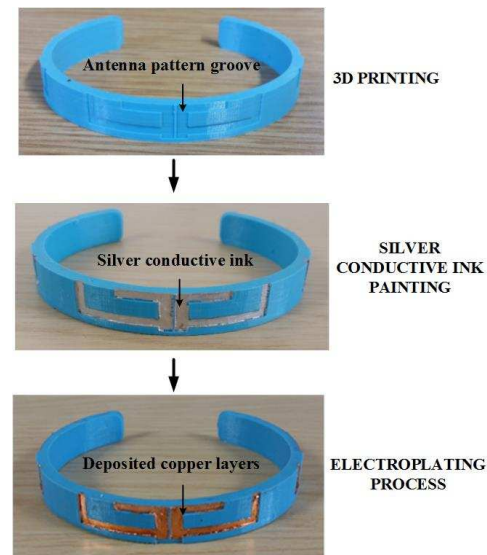


Fig. 12. Illustration of the first fabrication process for the diversity antenna system.

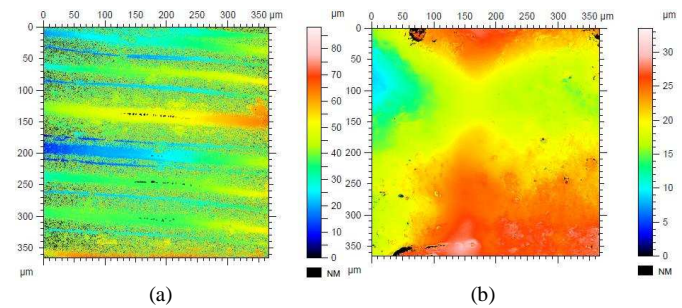


Fig.13. Surface profile map for (a) PLA substrate, and (b) copper layer.

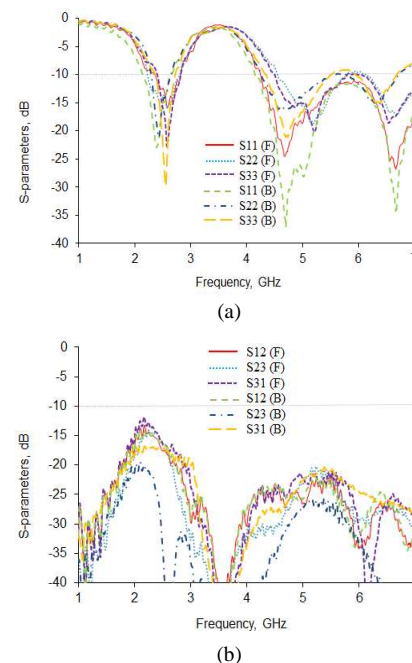


Fig. 14. Reflection coefficients (S_{11} , S_{22} , S_{33}) and correlation coefficients (S_{12} , S_{23} , S_{31}) of the diversity wrist worn antenna after electroplating process.

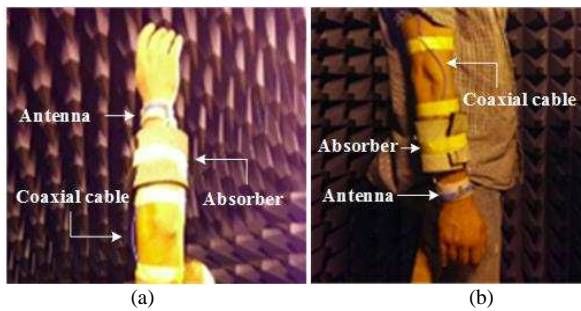


Fig. 15. Measurement setting in anechoic chamber for radiation patterns of the diversity wrist worn antenna after electroplating process with human wrist (a) Hand up (b) Hand down.

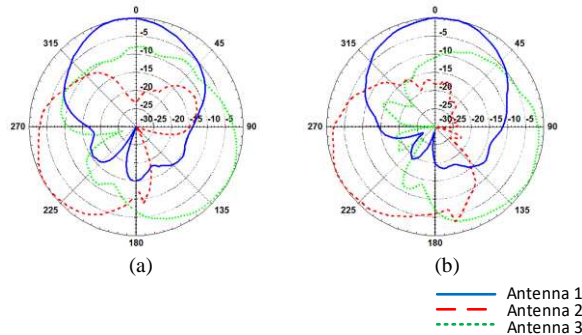


Fig. 16. Radiation patterns of the fist diversity wrist worn antennas fabricated by painting the ink layers (Hand up) at (a) 2.4 GHz (b) 5.5 GHz

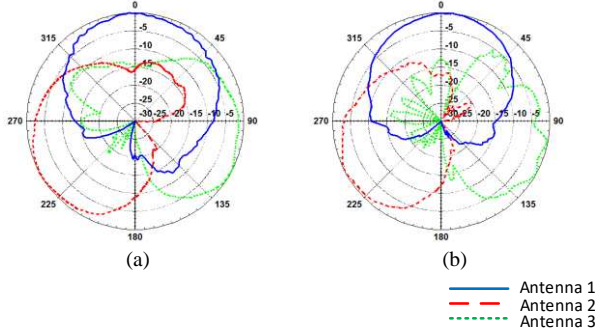


Fig. 17. Radiation patterns of the fist diversity wrist worn antennas fabricated by painting the ink layers (Hand Down) at (a) 2.4 GHz (b) 5.5 GHz.

Fig. 18 (b) shows the fully fabricated 3D printed diversity wrist worn antenna. Due to the nature of the bracelets' curvature and the required antenna on each side, the bracelet substrate was printed in two parts. One print was used for the frame of the bracelet substrate and the other to house the antennas. The frame of the bracelet was printed on a rigid, durable yellow PLA plastic filament from 3D FilaPrint [34], which had an infill of 100% and a layer resolution of 100 μ m. The thickness of this layer was 2 mm. The top layer of the bracelet was developed using a flexible PLA plastic filament from NinjaFlex [35]. The thickness of this layer was 1 mm. Immediately after printing this layer, the pneumatic dispenser printed the metallic tracks that make the antenna. The thicknesses of the metallic tracks were about 200 microns. A single layer of ink was enough to produce a resistance of less 0.4 Ohm between the two further ends of the dipole arms. Fig. 19 shows the surface profile of the printed layers. The surface roughness for the flexible PLA was about 11 μ m and the metallic ink layer of 2 μ m.

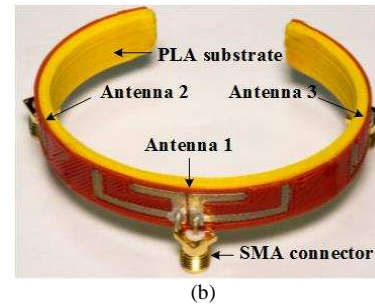
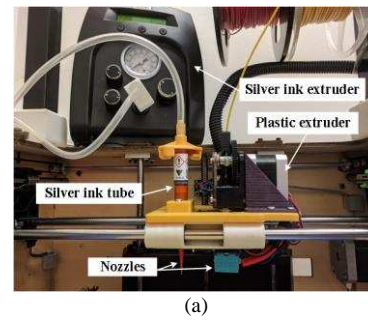


Fig. 18. Photograph of (a) used open-source 3D printer with dual extruders (b) Fabricated fully 3D printed diversity wrist wear antenna.

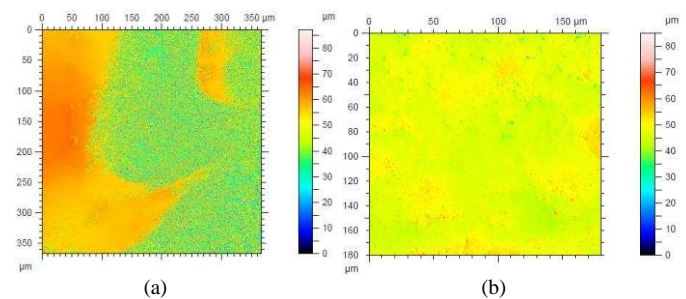


Fig. 19 Surface profile map for (a) flexible PLA substrate, and (b) conductive layer.

The flexible printed part with the antennas was mounted onto the rigid frame of the bracelet before the silver conductive ink had fully dried and cured. The two sections were then adhered together using double-sided tape with a thickness of 100 μ m.

The measured reflection S parameters of fully 3D printed diversity wrist worn antenna are shown in Fig. 20. In all tests, the 2.4 GHz and 5.5 GHz WLAN band were covered. The -10dB bandwidth ranges from 2.24 GHz to 3.14 GHz at the lower band and from 4.6 GHz to 7 GHz at the higher land.

Dipole antennas are well known for having unbalance ports. To suppress unbalanced surface current from the coaxial cable for the radiation measurement purpose, the probe-fed solution of the bazooka balun was applied to the antenna [36]. This was designed for the 2.4 GHz band. Fig. 21 shows the antenna system on the human wrist with the baluns.

Fig. 22 and Fig. 23 present the radiation patterns. It is evident that the human wrist provides backward signal attenuation. The radiation patterns are not any significantly different for two locations of human wrist such as hand up and hand down. The patterns were more directional on the human wrist than in free space. The use of baluns did not show a significant change in the patterns in the x-z plane compared to the straight measurements using coaxial feed.

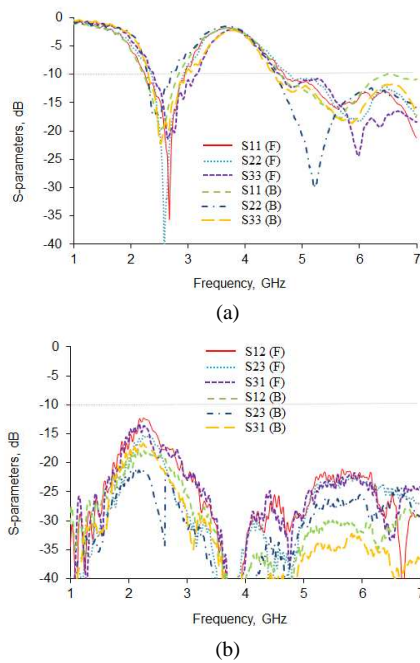


Fig. 20. Reflection coefficients (S_{11} , S_{22} , S_{33}) and correlation coefficients (S_{12} , S_{23} , S_{31}) of the fully 3D printed diversity wrist wear antenna.

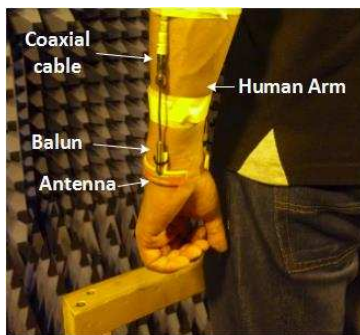


Fig. 21. Measurement setting in anechoic chamber for fabricated fully 3D printed diversity wrist wear antenna.

IV. DISCUSSIONS AND CONCLUSION

The additive manufacturing of conformal antennas onto a 3D printed wearable bracelet has been demonstrated. An antenna design suitable for the 2.4 GHz and 5.5 GHz WLAN bands has been employed. Three different AM procedures have been investigated. Table II shows the comparison between them. The first technique is a multistep process consisting on: 3D printing of the bracelet, deposition of a smoothing layer, aerosol jet printing of silver inks, flash curing, and electroplating with copper. The main advantages of this process are the high resolution of the printed antennas and the very smooth and thin metallic layer. The fact that it uses a range of machines means that it could become a chain process and therefore could be scaled up to a medium or even large industrial process. The main disadvantages are the many tasks involved in the fabrication and the cost of the equipment. Only one antenna can be printed in the bracelet fabricated unless a 3-axis deposition process is employed [22]. The second technique involves printing the bracelet with grooves and then painting the metallic layers of the antennas by hand. This process was able to

produce three antennas on the same bracelet with various conformal shapes.

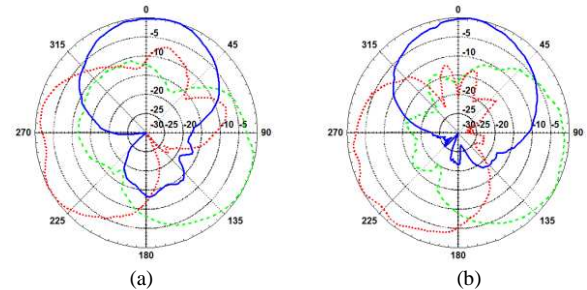


Fig. 22. Radiation patterns of the fully 3D printed diversity antenna with the human wrist (Hand up) at (a) 2.4 GHz (b) 5.5 GHz.

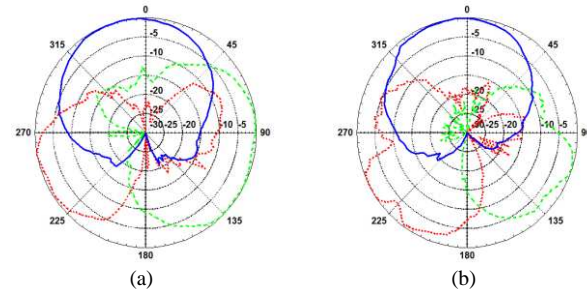


Fig. 23. Radiation patterns of the fully 3D printed diversity antenna with the human wrist and human body (Hand Down) at (a) 2.4 GHz (b) 5.5 GHz.

TABLE II
COMPARISON BETWEEN THE THREE FABRICATION METHODOLOGIES

Process	FDM+Aerosol Jet (Fig. 5)	FDM+Silver paint (Fig. 11)	FGM+Silver paste (Fig. 17)
Machine model	Ultimaker [37] + Optomec's Aerosol Jet	Ultimaker [37]+painted by hand	Open-source MBot 3D, Techcon TS250 dispenser.
Material	PLA + cyanoacrylate +silver ink + copper layer	PLA + silver conductive ink+ copper deposited layer	PLA + silver conductive paste (Voxel 8)
Metal layer thickness (μm)	70	100 – 200	200
Resolution	High	Low	Medium
Pros	Standard manufacture method, scalable	Low cost equipment, time saving for in-house prototyping	Low cost equipment, single step, time saving, scalable
Cons	High cost equipment, multi steps	Multi steps, Only suitable for prototyping	Require bending after fabrication
Bandwidth (Simulation, GHz)	2.28 - 2.63 4.79 - 6.12	2.28 - 2.63 4.79 - 6.12	2.28 - 2.63 4.79 - 6.12
Bandwidth (Measurement, GHz)	2.15 - 2.53 3.97 - 7	2.23 - 2.81 4.25 - 7	2.24 - 3.14 4.61 - 7

The main disadvantage is the errors related to the painting of the antennas by hand. This process is more suitable for small

scale production and prototyping unless the painting of the metallic tracks is carried out using an automatic procedure. The final process employs a single machine combining FFF for the fabrication of the bracelet and a pneumatic dispenser for the addition of the metallic layer using silver ink. A flexible PLA substrate has been used so that the antennas are printed in a planar form and then folded to create the bracelet. This has been proven to be the best manufacturing solution in terms of the number of tasks involved, the relative resolution of the printed tracks and the fact that is an automatic procedure. This could be scaled up to a medium industrial process. All processes described produced good results in terms of S_{11} and radiation pattern. These 3D printing techniques can be used for the fabrication of antennas and devices on bracelets customized to the user's wrist.

In terms of wireless communications, the use of three antennas on a bracelet has been demonstrated to be a good antenna diversity solution capable increasing coverage in wireless body area networks, particularly for off-body applications. These antennas could be used as part of a wireless location systems where each antenna is connected to its radio frequency (RF) circuit board and processor.

ACKNOWLEDGMENT

The author would like to thank Simon Jakes for help with fabrication. This work was funded by a UK EPSRC High Value Manufacturing Fellowship (REF: EP/L017121/1) and a RAEng Industrial Secondment scheme (REF: ISS1617/48).

REFERENCES

- [1] S. Upcraft and R. Fletcher, "The rapid prototyping technologies," *Assembly Autom.*, vol. 23, pp. 318–330, Jan. 2012.
- [2] H. Lipson and M. Kurman, *Fabricated: The New World of 3D Printing*. New York, NY, USA: Wiley, 2013.
- [3] N. Crane, J. Tuckerman, and G. N. Nielson, "Self-assembly in additive manufacturing: Opportunities and obstacles," *Rapid Prototyping J.*, vol. 17, no. 3, pp. 211–217, 2011.
- [4] J. Czyzewski, P. Burzynski, K. Gawel, and J. Meisner, "Rapid prototyping of electrically conductive components using 3D printing technology," *J. Mater. Process. Technol.*, vol. 209, no. 12–13, pp. 5281–5285, Jul. 2009.
- [5] B. Sanz-Izquierdo and E. Parker, "3-D Printing of Elements in Frequency Selective Arrays," *IEEE Trans. Antennas Propag.*, vol. 62, no. 12, pp. 6060–6066, 2014.
- [6] S. Y. Jun, B. Sanz-Izquierdo, E. A. Parker, D. Bird, and A. McClelland, "Manufacturing Considerations in the 3-D Printing of Fractal Antennas," *IEEE Trans. Compon. Packaging Manuf. Technol.*, vol. 7, pp. 1891–1898, 2017.
- [7] M. Liang, C. Shemelya, E. MacDonald, R. Wicker and H. Xin, "3-D Printed Microwave Patch Antenna via Fused Deposition Method and Ultrasonic Wire Mesh Embedding Technique," *IEEE Antennas Wirel. Propag. Lett.*, vol. 14, pp. 1346–1349, 2015.
- [8] I. T. Nassar and T. M. Weller, "Development of novel 3-D cube antennas for compact wireless sensor nodes," *IEEE Trans. Antennas Propag.*, vol. 60, pp. 1059–1065, 2012.
- [9] J. J. Adams et al., "Conformal printing of electrically small antennas on three-dimensional surfaces," *Adv. Mater.*, vol. 23, no. 11, pp. 1335–1340, Mar. 2011.
- [10] S. Jun, B. Sanz-Izquierdo, J. Heirons, C. Mao, S. Gao, D. Bird, and A. McClelland, "Circular polarised antenna fabricated with low-cost 3D and inkjet printing equipment," *Electron Lett.*, vol. 53, pp. 370–371, 2017.
- [11] B. Sanz-Izquierdo and S. Jun, "WLAN antenna on 3D printed bracelet and wrist phantom", in 2014 Loughborough Antennas and Propagation Conference (LAPC), 2014.
- [12] S. Jun, B. Sanz-Izquierdo, and M. Summerfield, "UWB antenna on 3D printed flexible substrate and foot phantom," in 2015 Loughborough Antennas and Propagation Conference (LAPC), 2015.
- [13] M. Rizwan, M. W. A. Khan, L. Sydänheimo, J. Virkki, and L. Ukkonen, "Flexible and Stretchable Brush-Painted Wearable Antenna on a Three-Dimensional (3-D) Printed Substrate," *IEEE Antennas Wireless Propag. Lett.*, vol. 16, pp. 3108–3112, 2017.
- [14] M. F. Farooqui and A. Shamim, "Dual band inkjet printed bow-tie slot antenna on leather," in *Antennas and Propagation (EuCAP)*, 2013 7th European Conference on, 2013, pp. 3287–3290.
- [15] W. G. Whittow, A. Chauraya, J. Vardaxoglou, Y. Li, R. Torah, K. Yang, S. Beeby, and J. Tudor, "Inkjet-printed microstrip patch antennas realized on textile for wearable applications," *IEEE Antennas Wireless Propag. Lett.*, vol. 13, pp. 71–74, 2014.
- [16] J. Winters, J. Salz and R. Gitlin, "The impact of antenna diversity on the capacity of wireless communication systems", *IEEE Transactions on Communications*, vol. 42, no. 234, pp. 1740–1751, 1994.
- [17] Lizhong Zheng and D. Tse, "Diversity and multiplexing: a fundamental tradeoff in multiple-antenna channels", *IEEE Trans. Inform. Theory*, vol. 49, no. 5, pp. 1073–1096, 2003.
- [18] C. Dietrich, K. Dietze, J. Nealy and W. Stutzman, "Spatial, polarization, and pattern diversity for wireless handheld terminals", *IEEE Trans. Antennas Propag.*, vol. 49, no. 9, pp. 1271–1281, 2001.
- [19] Z. Wang, L. Lee, D. Psychoudakis and J. Volakis, "Embroidered Multiband Body-Worn Antenna for GSM/PCS/WLAN Communications", *IEEE Trans. Antennas Propag.*, vol. 62, no. 6, pp. 3321–3329, 2014.
- [20] L. Akhondzadeh-Asl, I. Khan and P. Hall, "Polarisation diversity performance for on-body communication applications", *IET Microw. Antennas Propag.*, vol. 5, no. 2, p. 232, 2011.
- [21] R. Bharadwaj, S. Swaisaenyakorn, C. G. Parini, J. C. Batchelor, and A. Alomainy, "Impulse Radio Ultra-Wideband Communications for Localization and Tracking of Human Body and Limbs Movement for Healthcare Applications," *IEEE Trans. Antennas Propag.*, vol. 65, pp. 7298–7309, 2017.
- [22] M. Hedges, A. Borrás-Marin, "3D Aerosol jet printing - Adding electronics functionality to RP/RM", Neotech Services MTP.
- [23] I. T. Nassar, T. M. Weller, and H. Tsang, "A 3-D printed miniaturized log-periodic dipole antenna," in *Antennas and Propagation Society International Symposium (APSURSI)*, 2014 IEEE, 2014, pp. 11–12.
- [24] M. Mirzaee and S. Noghianian, "Additive manufacturing of a compact 3D dipole antenna using ABS thermoplastic and high temperature carbon paste," in *Antennas and Propagation (APSURSI)*, 2016 IEEE International Symposium on, 2016, pp. 475–476.
- [25] J.-S. Roh, Y.-S. Chi, J.-H. Lee, Y. Tak, S. Nam, and T. J. Kang, "Embroidered wearable multiresonant folded dipole antenna for FM reception," *IEEE Antennas Wireless Propag. Lett.*, vol. 9, pp. 803–806, 2010.
- [26] D. Sjöberg, A. J. Johansson and C. Larsson, "Electromagnetic properties of heterogeneous material structures produced in 3D-printers," 2014 International Conference on Electromagnetics in Advanced Applications (ICEAA), Palm Beach, 2014, pp. 605–607.
- [27] Federal Communications Commissions: Body tissue dielectric parameters, <http://www.fcc.gov/oet/rfsafety/dielectric.html>, C. Gabriel, "Compilation of the dielectric properties of body tissues at RF and microwave frequencies," Report N.AL/OE-TR- 1996-0037, Occupational and Environmental Health Directorate, Radiofrequency Radiation Division, Brooks Air Force Base, Texas, USA, June 1996
- [28] M. S. Alsoufi and A. E. Elsayed, "How Surface Roughness Performance of Printed Parts Manufactured by Desktop FDM 3D Printer with PLA+ is Influenced by Measuring Direction," *American Journal of Mechanical Engineering*, vol. 5, pp. 211–222, 2017.
- [29] [online] <https://www.novacentrix.com/> (Accessed 03/05/2018)
- [30] Centre for Process Innovation (CPI), <http://www.uk-cpi.com/> (Accessed 03/05/2018)
- [31] [online] <https://uk.rs-online.com/> (Accessed 03/05/2018)
- [32] [online] <http://www.mbot3d.com/> (Accessed 03/05/2018)
- [33] [online] <http://www.voxel8.com/> (Accessed 03/05/2018)
- [34] [online] <https://shop.3dfilaprint.com/> (Accessed 03/05/2018)
- [35] [online] <https://ninjatek.com/> (Accessed 03/05/2018)
- [36] M. Farooqui, C. Claudel and A. Shamim, "An Inkjet-Printed Buoyant 3-D Lagrangian Sensor for Real-Time Flood Monitoring", *IEEE Trans. Antennas Propag.*, vol. 62, no. 6, pp. 3354–3359, 2014.
- [37] [online]: <https://ultimaker.com/en/> (Accessed 03/05/2018)

